J Nanostruct 16(4): 5815-5823, Autumn 2026

RESEARCH PAPER

Development of Aptamer-Based Biosensors (Aptasensors) for Mycotoxin Detection

Ghadeer Huseen Al-Salihi *, Ali Al-Jawdah, Nassar Al-Esawy

Physics department, Science facility, University of Babylon, Iraq

ARTICLE INFO

Article History:
Received 10 June 2026
Accepted 15 September 2026
Published 01 October 2026

Keywords:
Aptamer
Biosensor
Mycotoxins
Nanoparticle
Plasmon

ABSTRACT

Mycotoxin pollution remains one of the most significant environmental problems. Dealing with this issue imposes providing proper detection equipment. In this work, an approach to improve the performance of optical biosensors is presented, particularly in terms of biosensitivity. Plasmon-based biosensors are leading the way in this field; however, much work remains to improve their performance. The LSPR chip uses metal nanoislands on glass made by thermal annealing. Interaction of light with these nanostructures causes resonance absorption at a specific wavelength. This results in an absorption spectrum with a peak at a specific wavelength. The resonant wavelength depends on the optical properties of the medium around the metallic nanoparticles; binding of biomolecules causes a red shift in the peak. Monitoring this shift is therefore the basis for sensing target biomolecules. Because accurate monitoring of the absorption peak is critical for biosensing. This work presents a method to improve the spectral shape, enabling more accurate detection of biomolecule-induced changes. The first thing engineers the setup to enhance the absorption peak. The second replaces conventional receptors, such as Protein A-antibody, with an aptamer-based thin bioreceptor layer, positioning the biomolecular binding within the stronger evanescent field. The results demonstrated a significant improvement in system performance over comparable systems, with enhanced sensitivity and reliability.

How to cite this article
Huseen Al-Salihi G., Al-Jawdah A., Al-Esawy N. Development of Aptamer-Based Biosensors (Aptasensors) for Mycotoxin Detection. J Nanostruct, 2026; 16(4):5815-5823. DOI: 10.22052/JNS.2026.04.110

INTRODUCTION

Mycotoxins are naturally produced by certain species of fungi and pose hazards to both environmental and human health [1-3]. Aflatoxin has been classified as one of the most potent natural carcinogens. Therefore, environmental and public health authorities have paid close attention to mitigating this threat. One of the most significant challenges in doing so is the difficulty of detection, especially at low concentrations, due to the small size of mycotoxin molecules. As a result, there is a growing demand for easy-to-use, portable devices capable of detecting low levels within safe limits and overcoming the challenges associated with this issue [4, 5].

In general, there are many trends in biosensing, each one of them functions based on a different sensing mechanism. The most commonly used is an optical type because of their sensitivity, specificity and fast response time [6, 7]. Local surface plasmon resonance is a phenomenon that has been employed for biosensing as optical

* *Corresponding Author Email: ghadeerhuseen75@gmail.com*

This work is licensed under the Creative Commons Attribution 4.0 International License.
To view a copy of this license, visit http://creativecommons.org/licenses/by/4.0/.

biosensor and has yielded ground breaking results. However, many aspects of this technique need development. This phenomenon occurs when electromagnetic light waves interact with nanoscale metal structures, where resonance absorption occurs at a specific wavelength. The optical properties of the medium surrounding metallic nanostructures determine the resonant wavelength. The presence of biomolecules within that medium can change these optical properties and thus shift the resonant wavelength. This phenomenon is used for biomolecular sensing by correlating the presence of target molecules to changes in the resonant absorption wavelength [8-10].

Metallic nanostructures are a key element in the development of plasmonic excitation. These nanostructures act as electrical dipoles Fig. 1, and when the natural frequency of the electron cloud's vibration matches the wavelength frequency of the incident light, resonant energy absorption occurs. This oscillation of the free electric charge called localized surface plasmon resonance (LSPR) [11-13].

This causes a loss of the resonant wavelength in the spectrum of the beam penetrating the nanostructure and the appearance of an absorption peak Fig. 2. The induced vibration of these electric charges generates an electromagnetic field called a plasmon field that extends and vanishes in both media surrounding the metallic structure. This phenomenon is interpreted theoretically by assuming; the metallic nanostructures are geometrically spheres with dimensions much less than the incident light wavelength ($R \ll \lambda$) [14].

According to this assumption, the electric field of the electromagnetic wave can be considered homogeneous through the assumed nanosphere, in this case, the electro-static mode can be apply for this condition.

The electric field of the light wave attempts to polarize the free charge in the nanoparticles. Since the electric field is oscillating, the electron cloud will induce oscillation. During this interaction, energy is transferred from the waves to the electron cloud, and maximum energy transfer reached when the wave frequency equals the natural vibrational frequency of the electron cloud [15,16].

The dipole system is characterized by a polarizability which represents the response of the dipole to an external electric field that can be mathematically determined using boundary conditions.

The dipole system is characterized by a polarizability α which represents the response of the dipol to an external electric field, which can be mathematically calculated using Laplace equation and conceder the boundary condition [17, 18]:

$$\alpha = 4\pi R^3 \frac{\varepsilon_{(\omega)} - \varepsilon_d}{\varepsilon_{(\omega)} + 2\varepsilon_d} \quad (1)$$

Clearly, the value of polarizability α indicates to ability of the nanostructure of absorbing electromagnetic energy.

Eq. 2 indicates that when:

$$\varepsilon_1(\omega) = -2\varepsilon_d. \quad (2)$$

The greatest energy absorption will be happen, which represents the state of plasmon resonance. The dielectric constant of a metal is a function of wavelength; therefore, at a given wavelength, the Eq. 2 will satisfy, and a surface plasmon will be excited, this called Frölich condition. For most noble metals, this resonance wavelength in rang of visible spectrum. Therefore, noble metals are proper material to establish the plasmon phoneme [19]. Equation (1) shows that the polarizability is affected by the dielectric constant of the surrounding medium, which is related to the refractive index n of the surrounding medium, so that any change in the refractive index of the medium within the evanescent field range leads to modification of the polarizability and a shift of the LSPR peak. Based on that, this system was adopted to sense changes in the optical properties of the surrounding medium.

For a specific system of nanostructures made of a given metal, the polarizability α is a function of the dielectric constant of the surrounding medium [20].

$$\alpha = \alpha_{(\epsilon_d)} \quad (3)$$

$$\epsilon_d = n^2 \quad (4)$$

$$\alpha = \alpha(n) \quad (5)$$

The correlation between the position of the absorption peak and the optical properties of the surrounding medium forms the basis for this system's operation as a sensor.The presence of

CC BY

biomolecules alters the surrounding environment, leading to changes in the optical properties of the medium around the nanostructures and, consequently, to a shift in the plasmonic resonance wavelength.To link the change in plasmonic resonance wavelength to specific biomolecules, a bioreceptor layer is immobilized on the metallic nanostructures. This layer selectively binds target biomolecules, ensuring that only the targeted analytes affect the sensing region.

The change in optical properties is reflected in the change in the refractive index of the medium. The relationship between the change in refractive index and the resulting resonant wavelength shift is modeled by the following expression [21, 22]:

$$\Delta\lambda = m(\Delta n)[1 - \exp\left(\frac{-2d}{l_d}\right)] \quad (6)$$

m is the refractive index sensitivity, Δn is the change in refractive index induced by the adsorbate, d is the effective adsorbate layer thickness and l_d is the electromagnetic field decay length (approximated as an exponential decay).

According to the equation, the magnitude of the absorption peak shift depends on two factors: 1) the change in refractive index, which is determined by the type of bound biomolecule, and 2) the thickness of the binding layer, which corresponds to the density or concentration of target molecules

One of the most important performance criteria for sensors is sensitivity, defined as the ratio of the change in the output signal to the change in the measured quantity. An LSPR biosensor is an optical-based sensor that detects biomolecules by monitoring changes in their optical signature. Therefore, to evaluate its biosensing performance, optical sensitivity must first be assessed. Optical sensitivity is defined as the absorption peak shift (nm) per unit change in the refractive index of the medium (RIU). Biosensitivity is then defined as the absorption peak shift (nm) per unit change in the concentration of the target molecules [23, 24].

MATERIALS AND METHODS

Experimental LSPR biosensing

Fabrication of Au NPs platform

This experiment consists of three main elements; spectrometer, LSPR chip and light source. The LSPR chips were formed by depositing a thin layer of gold on (20 X 20 mm) BK7 glass substrates. The successful depositing of metallic films onto glass slides requires deep and effective pre-cleaning. For this purpose: first slides were rinsed by distilled water to remove large particles and dust, then, immersed in alcohol (high-purity ethanol) for 15 min to remove organic impurities. The acidity of final rinse water was tested to ensure it is around 7, otherwise, the rinse is repeated until the acidity level is reached 7. Finally, the drying process was carried out using flow of dry air. These cleaned slides were coated with an initial 2 nm thin layer of chrome as an adhesion layer. Then, different thicknesses (10, 15, 20, 25 and 50 nm) have been deposed using magnetron sputtering technology (MTI Corporation GSL-1100X-SPC-16M). Thickness was determined from deposition time using a calibration curve.

To convert the flat gold thin films to Nano islands, they subjected to heat treatments using a convection furnace, they subject to gradually heated up to 450 degrees for 5 hours, followed by gradual cooling. The SEM (FEI-Nova, Nano SEM 200) images show that the flat gold thin films have dewetted to form nano islands Fig. 2.

RESULTS AND DISCUSSION

Statistical checking suggests that thickness 20 nm exhibits the most homogeneity, produce

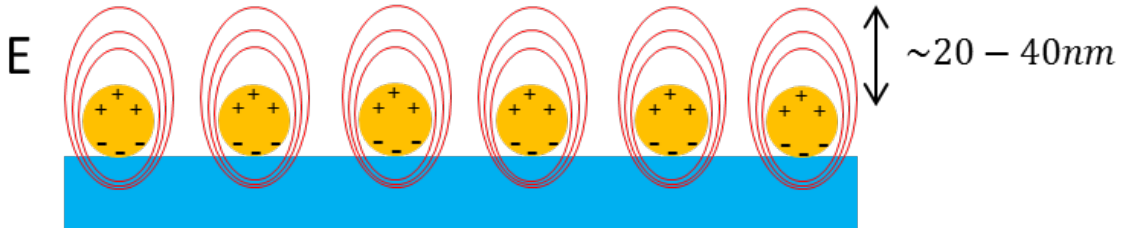


Fig. 1. Evanescent field of LSPR.

CC BY

Nano-islands with dimensions of approximately 50 nm for approximately 50%. Therefore, 20 nm thickness has been was adopted to establish the plasmon phenomenon.

A nylon microfluidic cell Fig. 4. was designed and implemented to contain the LSPR chip and making it into contact with the liquid solutions. The cell has a cavity equipped inlet and outlet micro piping allow injection solutions using electric syringe to ensure a rate controlled and smooth flow.

In addition, the cell was equipped with two opposing quartz windows to allow light transmission through the cell, the nanostructured film, and the solution. Illumination was provided by a broadband light source (tungsten lamp, 20W) coupled by optical fiber covering spectral range of 300–800 nm. Transmitted light was collected using an Ocean Optics FLAME-S-XR1 spectrometer, and absorption spectra were acquired and processed using OceanView software. Localized surface plasmon resonance was excited with this configuration, and the corresponding LSPR spectra were recorded as depicted in Fig. 5. The resulted spectrums were characterized by specific peaks for each thickness that confirm the phenomenon of local plasmon resonance has been happen.

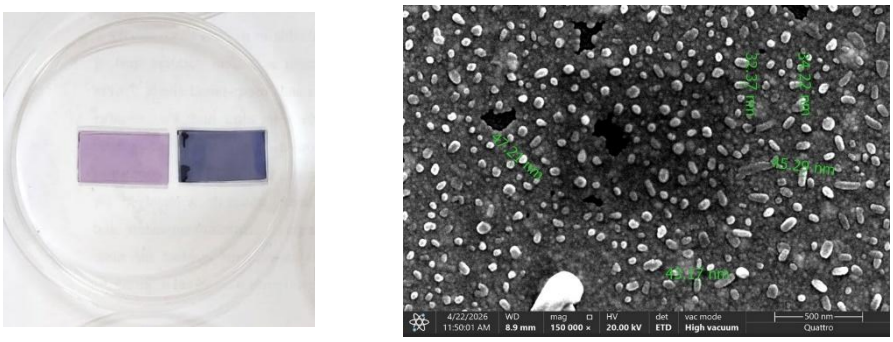


Fig. 2. Gold thin films before and after annealing (a), SEM image (b).

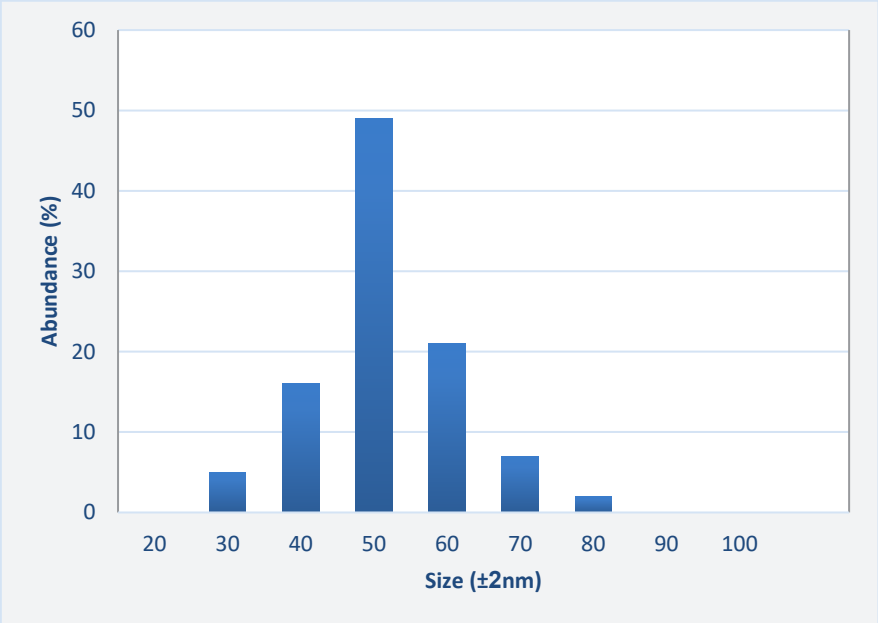


Fig. 3. Size distribution of the Au thin film Nanostructure.

To enhance sensing resolution, the FWHM of the absorption peak must be minimized. Here, an event-repetition strategy was adopted to improve LSPR spectral quality, using a suggested arrangement shown in Fig. 6.

A reflector system was used to pass the incident beam through the plasmonic structure three times, effectively replicating the excitation. This resulted in a 30% reduction in FWHM." Fig. 7.

The optical performance of the system was evaluated by measuring its response to changes in the refractive index of the medium using standard

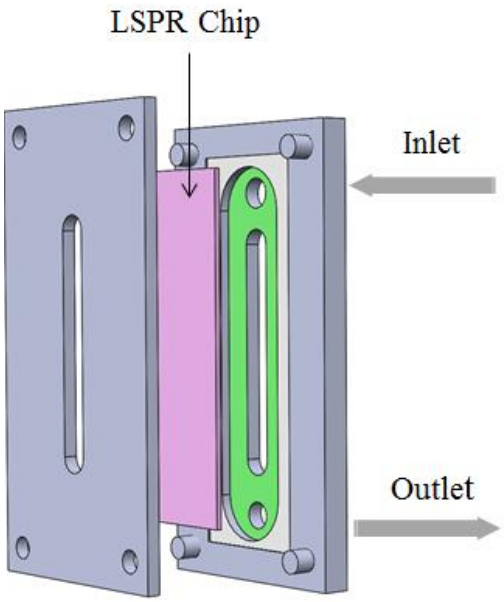


Fig. 4. Microfluidic cell.

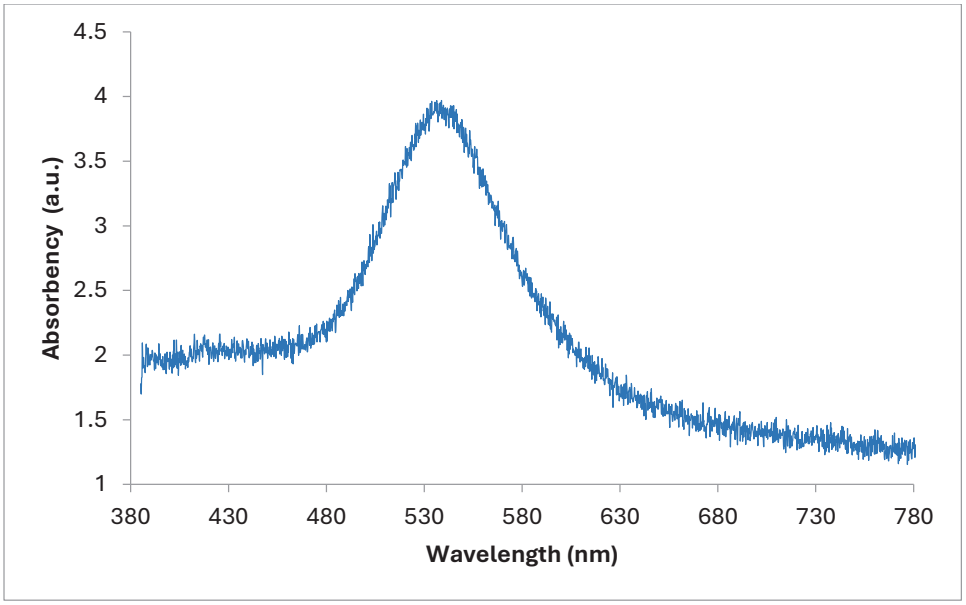


Fig. 5. LSPR Spectrum.

CC BY

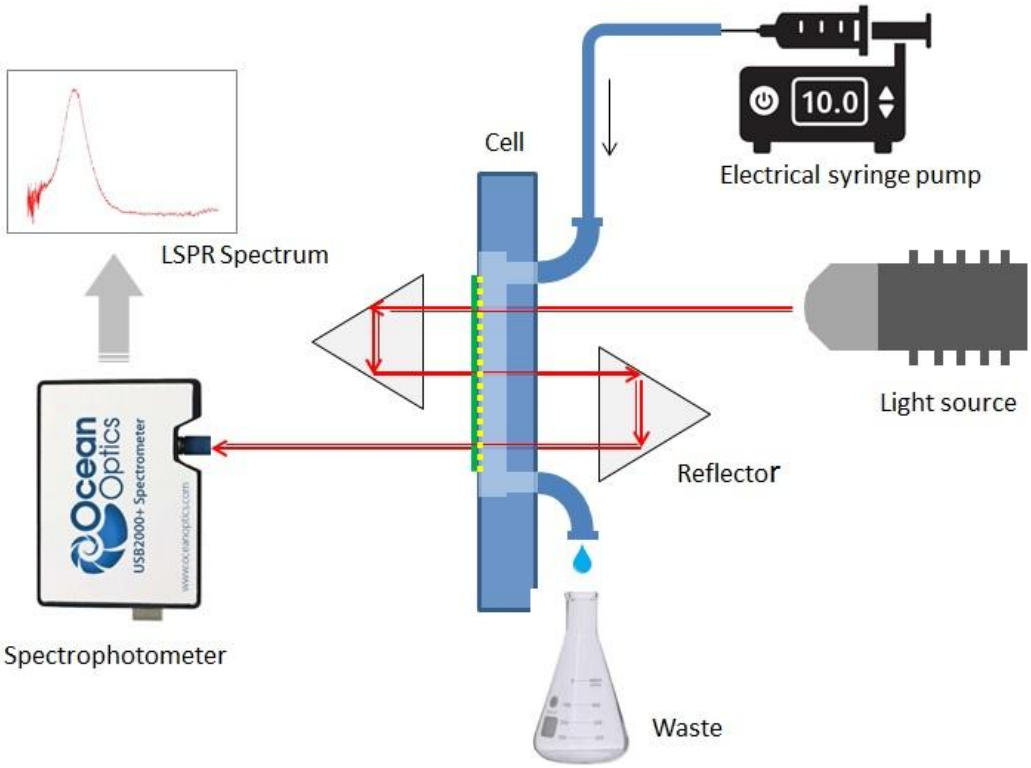


Fig. 6. LSPR setup utilizing multiple reflections to induce more than one plasmon event.

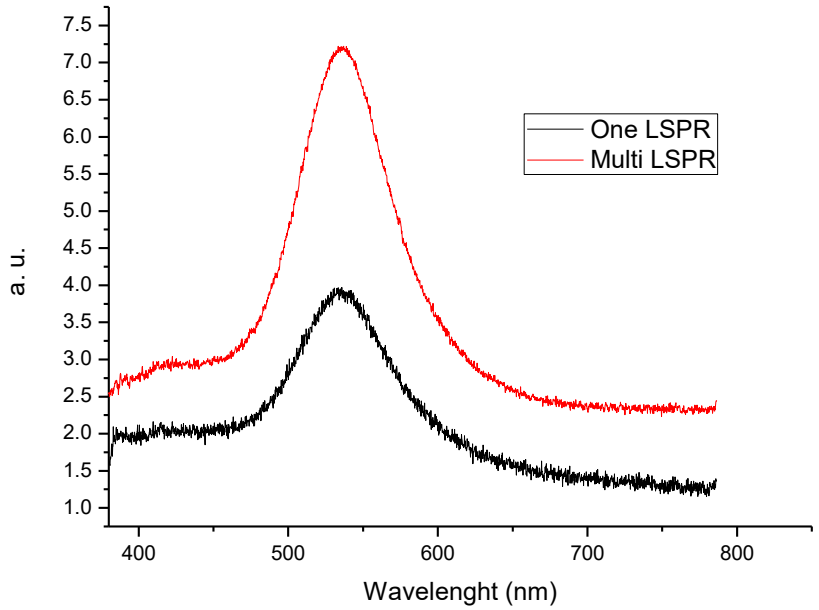


Fig. 7. LSPR plasmon spectrum using multi event set up.

CC BY

refractive index solutions. The results showed the refractive index sensitivity (RIS) of the system in range of 529nm/RIU Fig. 8. This value was deemed sufficient to move forward with employing the system for biosensing.

To overcome the shortcomings of previous works, which were due to the limited of LSPR evanescent field (<50 nm), aptamer was employed as a bioreceptor. The immobilization was carried out by mixing the original solution (100 µM) with 2 mM of 1,4-Dithiothreitol in HEPES buffer, to remove the protection group and release the

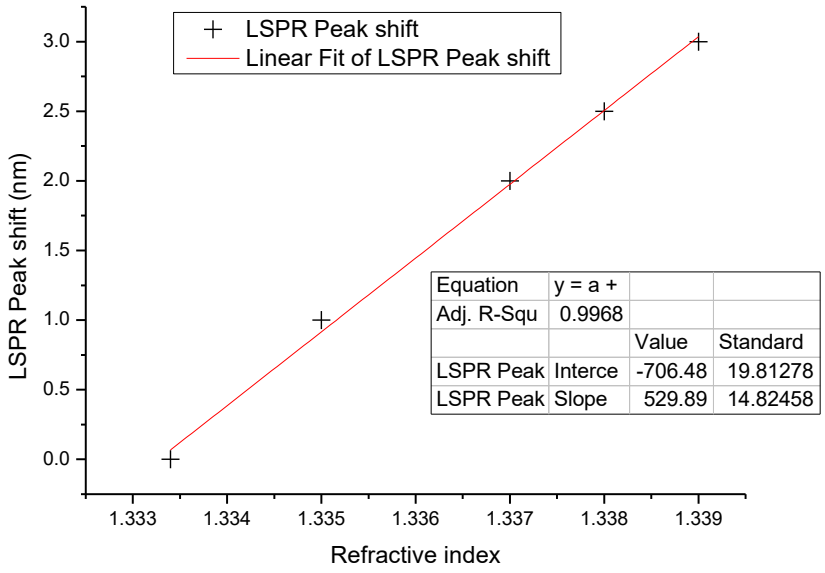


Fig. 8. RIU sensitivity Calibration.

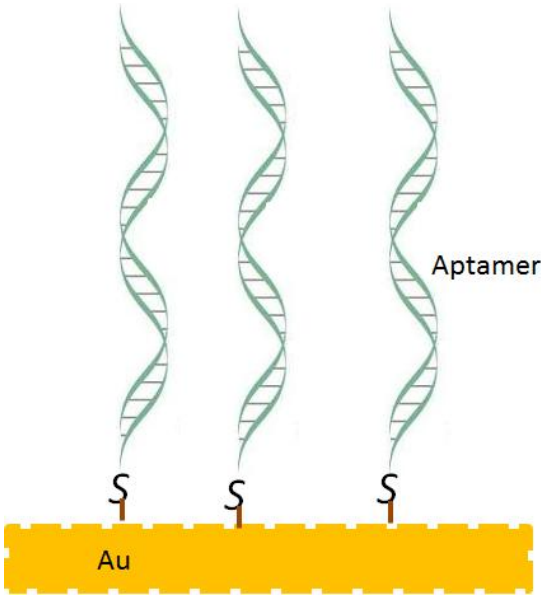


Fig. 9. Aptamer immobilization via thiol group (self-assembled monolayers).

CC BY

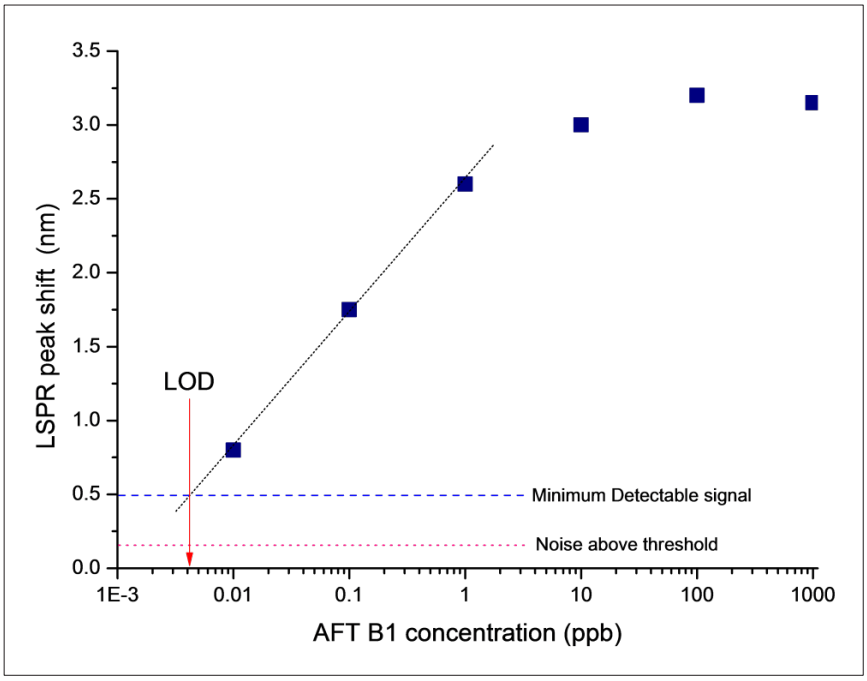


Fig. 10. LSPR peak shift as a function of aflatoxin concentration.

aptamers, 2mM of MgCl2 was supplement. The aptamers were functionalized with thiol group (C3-SH) to obtain strong binding to gold Fig. 9.

Biosensing

Aflatoxin B1 (AFB1) stander solution (1mg/mL) was diluted in acetonitrile. Further dilutions in PBB buffer were made to prepare several concentrations. All working concentration of 0.01 ng/mL, 1 ng/mL, 10 ng/mL, 100 ng/mL, and 1 µg/mL have been prepared and kept at 5 °C until they were time to use them in the sensing test. Intermediate washing of the cell by inject it with 1 mL of PBB solution was done after each concentration measurement in order to remove non-specifically bind toxin molecules.

The spectrums were recorded after binding of AFT B1to their specific aptamer which take time approximately 20 min to complete the binding.

The shift in the absorption peak position in the spectra was detected, as the result shown in Fig. 10. When AFB1 molecules were embraced by the receptor the RI near Au nanostructure changes, resulting in shifting of the peak position as shown in Fig. 10, the relationship between Δλ and AFB1 concentration is non-linear. After logarithmic transformation of the concentration values, an initial linear response was observed, followed by the onset of saturation. This saturation is attributed to the occupancy of all available receptor binding sites.

The sensing response had a linear range of 0.01 to 1 ppb, the LOD was determined by linear extrapolation of the linear fitting of linear part down to three times the noise level. The intersection point corresponds to the limit of detection of the sensor, which was 0.003 ppb. The results show that the lowest detectable increment is a 0.003 ng/mL. Which indicates the sensing chip is exhibited proper sensitivity.

CONCLUSION

A set up of local surface plasmon resonance chip with a microfluidic cell and an optical coupling platform were developed for Aflatoxin B1 detection. Metal nanostructures were prepared by depositing thin film of gold on glass and then convert it to Nano-island structure by specific heat treatment. The optical performance test showed a high degree of refractive index sensitivity which encourage to employed it to the detect small biomolecules. Utilization of plasmonic event

CC BY

repetition has been successfully enhanced the spectrum curve, thus developing the bio sensitivity and limit of detection, which is as sensitive as 100ng and 100 gm respectively. In conclusion, work has demonstrated this simple approach based on repeating LSPR has enhanced performance in mycotoxin detection. Further development is possible to meet the global demand in this issue.

CONFLICT OF INTEREST

The authors declare that there is no conflict of interests regarding the publication of this manuscript.

REFERENCES

1. Richard JL. Some major mycotoxins and their mycotoxicoses—An overview. Int J Food Microbiol. 2007;119(1-2):3-10.
2. Zain ME. Impact of mycotoxins on humans and animals. Journal of Saudi Chemical Society. 2011;15(2):129-144.
3. Steyn PS. Mycotoxins, general view, chemistry and structure. Toxicol Lett. 1995;82-83:843-851.
4. Deng J, Zhao M, Jiang H. Research Progress in the Detection of Mycotoxins in Cereals and Their Products by Vibrational Spectroscopy. Foods. 2025;14(15):2688.
5. Singh J, Mehta A. Rapid and sensitive detection of mycotoxins by advanced and emerging analytical methods: A review. Food Science and Nutrition. 2020;8(5):2183-2204.
6. Damborský P, Švitel J, Katrlík J. Optical biosensors. Essays Biochem. 2016;60(1):91-100.
7. Chen C, Wang J. Optical biosensors: an exhaustive and comprehensive review. The Analyst. 2020;145(5):1605-1628.
8. Mayer KM, Hafner JH. Localized Surface Plasmon Resonance Sensors. Chem Rev. 2011;111(6):3828-3857.
9. Willets KA, Van Duyne RP. Localized Surface Plasmon Resonance Spectroscopy and Sensing. Annu Rev Phys Chem. 2007;58(1):267-297.
10. Zhao J, Zhang X, Yonzon CR, Haes AJ, Van Duyne RP. Localized Surface Plasmon Resonance Biosensors. Nanomedicine. 2006;1(2):219-228.
11. McOyi MP, Mpofu KT, Sekhwama M, Mthunzi-Kufa P. Developments in Localized Surface Plasmon Resonance. Plasmonics. 2024;20(7):5481-5520.
12. Zhang Y, He S, Guo W, Hu Y, Huang J, Mulcahy JR, et al. Surface-Plasmon-Driven Hot Electron Photochemistry. Chem Rev. 2017;118(6):2927-2954.
13. Sotnikov DV, Zherdev AV, Dzantiev BB. Detection of Intermolecular Interactions Based on Surface Plasmon Resonance Registration. Biochemistry (Moscow). 2015;80(13):1820-1832.
14. Halas NJ, Lal S, Chang W-S, Link S, Nordlander P. Plasmons in Strongly Coupled Metallic Nanostructures. Chem Rev. 2011;111(6):3913-3961.
15. Krajczewski J, Kołątaj K, Kudelski A. Plasmonic nanoparticles in chemical analysis. RSC Advances. 2017;7(28):17559-17576.
16. Wang L, Hasanzadeh Kafshgari M, Meunier M. Optical Properties and Applications of Plasmonic-Metal Nanoparticles. Adv Funct Mater. 2020;30(51).
17. Ghosh SK, Pal T. Interparticle Coupling Effect on the Surface Plasmon Resonance of Gold Nanoparticles: From Theory to Applications. Chem Rev. 2007;107(11):4797-4862.
18. Kelly KL, Coronado E, Zhao LL, Schatz GC. The Optical Properties of Metal Nanoparticles: The Influence of Size, Shape, and Dielectric Environment. The Journal of Physical Chemistry B. 2002;107(3):668-677.
19. Lazarides AA, Lance Kelly K, Jensen TR, Schatz GC. Optical properties of metal nanoparticles and nanoparticle aggregates important in biosensors. Journal of Molecular Structure: THEOCHEM. 2000;529(1-3):59-63.
20. Zhou J, Wang Y, Zhang L, Li X. Plasmonic biosensing based on non-noble-metal materials. Chin Chem Lett. 2018;29(1):54-60.
21. Anker JN, Hall WP, Lyandres O, Shah NC, Zhao J, Van Duyne RP. Biosensing with plasmonic nanosensors. Nature Materials. 2008;7(6):442-453.
22. Ziegler C, Göpel W. Biosensor development. Curr Opin Chem Biol. 1998;2(5):585-591.
23. Kirsch J, Siltanen C, Zhou Q, Revzin A, Simonian A. Biosensor technology: recent advances in threat agent detection and medicine. Chem Soc Rev. 2013;42(22):8733.

CC BY